doi:10.1016/j.jmb.2010.02.024 J. Mol. Biol. (2010) 397, 1188–1198

JMB

Available online at www.sciencedirect.com

ScienceDirect

ELSEVIER

Mutations in Desmin's Carboxy-Terminal "Tail" Domain Severely Modify Filament and Network Mechanics

Harald Bär[1,2]†, Michael Schopferer[3]†, Sarika Sharma[1,2], Bernhard Hochstein[3], Norbert Mücke[4], Harald Herrmann[2] and Norbert Willenbacher[3]*

[1]*Department of Cardiology, University of Heidelberg, 69120 Heidelberg, Germany*

[2]*Group Functional Architecture of the Cell, German Cancer Research Center, 69120 Heidelberg, Germany*

[3]*Institute of Mechanical Process Engineering and Mechanics, University of Karlsruhe, Gotthard-Franz-Straße 3, 76131 Karlsruhe, Germany*

[4]*Division of Biophysics of Macromolecules, German Cancer Research Center, 69120 Heidelberg, Germany*

Received 25 August 2009; received in revised form 25 January 2010; accepted 12 February 2010
Available online 18 February 2010

Inherited mutations in the gene coding for the intermediate filament protein desmin have been demonstrated to cause severe skeletal and cardiac myopathies. Unexpectedly, some of the mutated desmins, in particular those carrying single amino acid alterations in the non-α-helical carboxy-terminal domain ("tail"), have been demonstrated to form apparently normal filaments both *in vitro* and in transfected cells. Thus, it is not clear if filament properties are affected by these mutations at all. For this reason, we performed oscillatory shear experiments with six different desmin "tail" mutants in order to characterize the mesh size of filament networks and their strain stiffening properties. Moreover, we have carried out high-frequency oscillatory squeeze flow measurements to determine the bending stiffness of the respective filaments, characterized by the persistence length l_p. Interestingly, mesh size was not altered for the mutant filament networks, except for the mutant *Des*R454W, which apparently did not form proper filament networks. Also, the values for bending stiffness were in the same range for both the "tail" mutants ($l_p = 1.0–2.0$ μm) and the wild-type desmin ($l_p = 1.1 \pm 0.5$ μm). However, most investigated desmin mutants exhibited a distinct reduction in strain stiffening compared to wild-type desmin and promoted nonaffine network deformation. Therefore, we conclude that the mutated amino acids affect intrafilamentous architecture and colloidal interactions along the filament in such a way that the response to applied strain is significantly altered.

In order to explore the importance of the "tail" domain as such for filament network properties, we employed a "tail"-truncated desmin. Under standard conditions, it formed extended regular filaments, but failed to generate strain stiffening. Hence, these data strongly indicate that the "tail" domain is responsible for attractive filament–filament interactions. Moreover, these types of interactions may also be relevant to the network properties of the desmin cytoskeleton in patient muscle.

Keywords: modifications in desmin filament and network mechanics due to mutations; electron microscopy; rheology; persistence length; strain stiffening

Edited by M. Moody

Introduction

In animal cells, microfilaments, microtubules, and intermediate filaments (IFs) constitute a dense, tightly interconnected cytoplasmic filament network.[1] Mutations in the gene coding for the muscle-specific IF protein desmin cause desminopathy, a subset of myofibrillar myopathy. This severe muscle disease can affect both skeletal and cardiac muscles.[2–4] One hypothesis raised previously was that these mutations would render the mutant desmin protein assembly incompetent and would consecutively cause the misfolded protein to be segregated into large intracellular aggregates—the characteristic histological finding in affected muscle.[5] However, this theory may have to be modified and extended, as

*Corresponding author. E-mail address: norbert.willenbacher@kit.edu.

† H.B. and M.S. contributed equally to this work.

Abbreviations used: IF, intermediate filament; PBS, phosphate-buffered saline.

extensive analyses involving recombinant wild-type and mutant desmin proteins and transfection studies in several cell lines revealed that part of the mutations does not impair the filament assembly of the respective mutant desmin variants both *in vitro* and *in vivo*.[6–8] In particular, mutations residing in desmin's carboxy-terminal non-α-helical "tail" domain were shown to be mostly assembly competent.[9] These findings immediately offer a more complex model of the development of disease in desminopathy: mutant desmin variants that allow filament formation are now believed to impact on desmin function at a higher-order level, either by altering the "intrinsic" biophysical properties of the filament itself or by changing binding properties towards associated proteins ("extrinsic" filament properties).[1] The former hypothesis has only recently gained support from investigations on the nanomechanical properties of individual desmin IFs through stress measurements using the tip of the cantilever of an atomic force microscope.[10] Just as well, the latter hypothesis was strengthened substantially through the finding that the assembly-competent desmin mutant *Des*E245D alters the interaction of desmin with nebulin and thereby directly influences microfilament architecture.[11]

The focus of the present study was to analyze the impact of mutations in the carboxy-terminal non-α-helical "tail" domain of desmin on the biophysical properties of filament networks in bulk solution. These mutations were chosen as we could recently demonstrate that all of them assembled into filaments both *in vitro* and in transfected myoblasts, although with different efficiencies.[9] As the observed disease phenotype in patients carrying these mutations is as severe as that for mutations that render the desmin protein completely assembly incompetent, part of the mechanisms underlying the development of severe myopathy may lie in alterations in the properties of filaments due to single amino acid exchanges. Accordingly, it has been pointed out earlier that mutations in another IF system (i.e., keratins) can alter the mechanical properties of their networks substantially.[12] Especially, the non-α-helical tail domain has been shown to have a strong impact on the bundling and strain stiffening of keratin networks.[13,14] However, the assembly reaction of keratins, forming complex networks in epithelia, differs considerably from that of IF proteins such as vimentin and desmin.[15] Hence, under conditions where vimentin and desmin do not organize above tetramers and octamers, keratins assemble into huge networks; moreover, keratin IFs have a tendency to bundle massively,[14] a property not observed with vimentin and desmin even at high protein and salt concentrations.[16] Therefore, the detailed interactions of keratins and desmin, respectively, in higher-order networks are certainly quite different.

In order to test the hypothesis that desmin "tail" mutations cause alterations in "intrinsic" filament properties, we employed conventional mechanical rheometry, as well as high-frequency oscillatory shear experiments, to characterize the biophysical properties of filament networks formed by the respective recombinant mutant proteins. Recent analyses of the viscoelastic properties of both wild-type desmin and vimentin filament networks illustrated the potential of these techniques to characterize the viscoelastic mechanical properties of these "biopolymers" in solution.[16] Oscillatory shear experiments at constant frequency and varying stress amplitudes have been used to characterize the mesh size and strain stiffening properties of the filament network, while the bending stiffness of individual filaments in solution has been deduced from small-amplitude high-frequency oscillatory squeeze flow measurements. In order to understand the influence of the "tail" domain as such on the filament's viscoelastic properties in detail, we additionally analyzed a tail-deleted desmin variant.

Our findings show that the tail domain is indeed important for establishing desmin's characteristic mechanical filament properties and that mutations can significantly change "intrinsic" filament properties without altering the filament morphology, as revealed by high-resolution electron microscopy. Given the important role that desmin IFs play as mechanosensor and mechanotransducer within myocytes, we speculate that these profound alterations in the nanomechanical properties of desmin have clinical relevance and might contribute to disease development.

Results and Discussion

Filament assembly *in vitro*

In order to visualize the polymerized mutant desmin variants analyzed by rheometry, we have assembled the respective proteins at the concentration employed in rheological experiments (i.e., at 1.0 g/l). After fixation and dilution of the samples to 0.1 g/l, filaments were negatively stained, and filament width was measured by electron microscopy. The tail-truncated desmin variant (*Des*ΔTail) is capable of forming *bona fide* IFs, which, when compared to wild-type desmin (*Des*WT), are slightly more irregular (Fig. 1a) but of similar diameter (Table 1). As previously documented,[9] all mutant desmin variants, except for *Des*R454W, are able to form extended filamentous networks. Assemblies of *Des*R454W exhibit defective longitudinal annealing properties and, thus, only short filamentous structures were observed (Fig. 1b). Upon copolymerization with an equimolar ratio of wild-type desmin, most mutants are capable of filament formation. Quite remarkably, however, the equimolar mixture of *Des*K449T and wild-type protein performed rather poorly, as relatively short and irregular filaments of varying lengths were formed (Fig. 1c, left). Obviously, this mutant exerts a dominant-negative effect on wild-type desmin assembly, thus causing both defective longitudinal elongation and

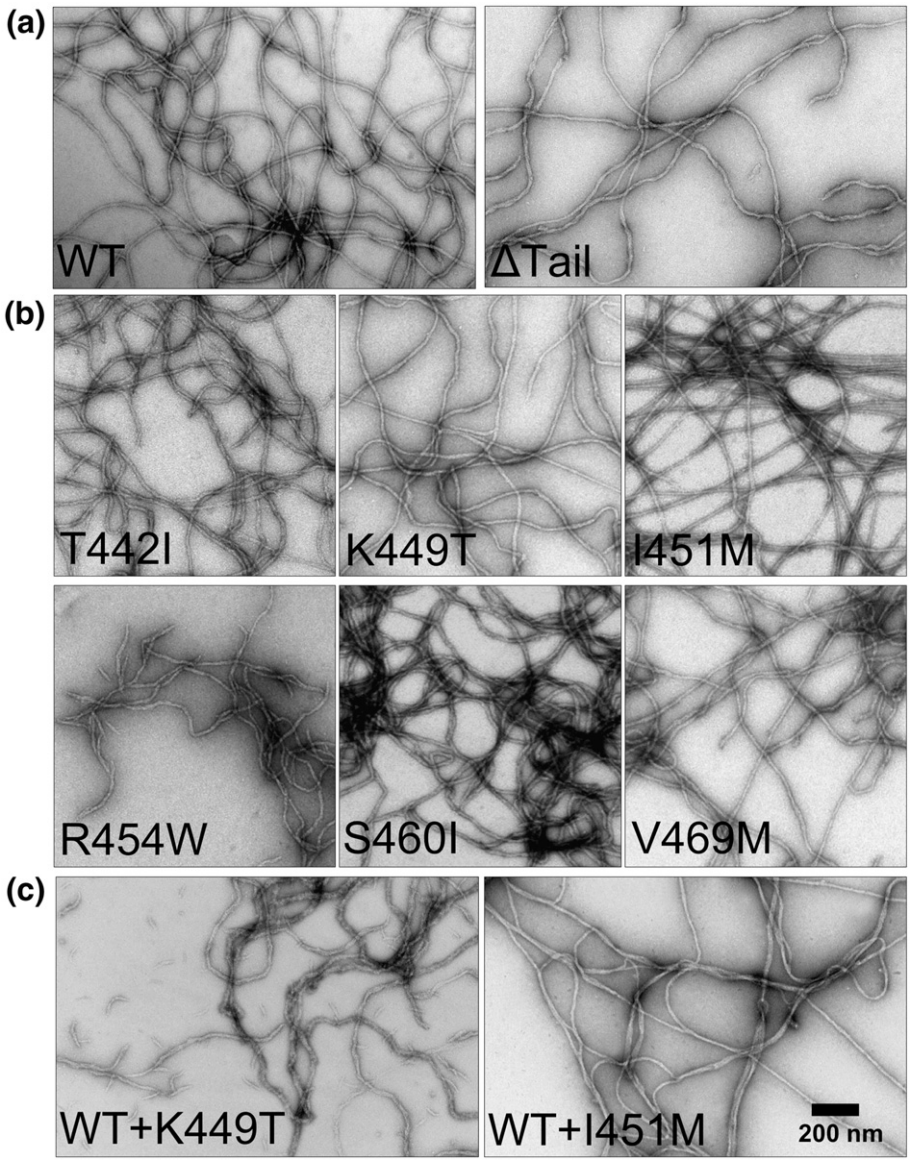

Fig. 1. (a) Electron microscopic analyses of negatively stained assemblies of wild-type desmin and *Des*ΔTail. Assembly was at 1.0 g/l for 60 min. Note that *Des*ΔTail assembles into more irregular filaments. (b) Negatively stained assemblies of *Des*T442I, *Des*K449T, *Des*I451M, *Des*R454W, *Des*S460I, and *Des*V469M. Note that *Des*R454W only assembles into short filamentous structures, whereas all other mutants are able to form extended filamentous networks. (c) Assemblies of equimolar mixtures of wild-type desmin with the mutants *Des*K449T and *Des*I451M, respectively. Note that in the heteropolymeric situation, *Des*K449T no longer assembles into extended filamentous networks. Instead, short unit length filament-like structures indicate a disturbed longitudinal annealing potential of heteropolymers. In addition, longer but highly irregular filaments point to altered radial compaction properties. These findings prove that the mutant protein does exert a dominant-negative effect on wild-type desmin assembly. Scale bar represents 200 nm.

disturbed radial compaction of the filaments.[9] For *Des*I451M, lateral fusion of single filaments and filament bundle formation were observed during coassembly with wild-type desmin (Fig. 1c, right).

As previously shown, filament diameter corresponds to the number of molecules per cross section.[8] Filament width measurements obtained for the assembled proteins revealed filament diameters between 12.2 nm and 16.5 nm (Table 2), indicating the potential of single amino acid exchanges in the tail domain of desmin to substantially alter the intrafilamentous architecture.

Filament assembly *in vivo*

In order to reveal if these *in vitro* assembly and network properties were also principally recapitulated in live cells, we analyzed the assembly properties of the mutant desmin proteins in two cellular backgrounds that proved to be optimal for the analysis of the capacity of desmin mutants to assemble into proper IF networks. First, we employed primary embryonic fibroblast cells obtained from vimentin knockout mice (MEF $Vim^{-/-}$) that are completely devoid of endogenous

Table 1. Filament diameters, mesh sizes, and drag coefficients

Protein	Filament diameter[a] d_f (nm)	Mesh size[a] ξ (nm)	Drag coefficient[a] ζ (10^{-3} N s/m^2)
Wild-type desmin (*Des*WT)	12.9	200	4.0
*Des*ΔTail	13.4	165	4.4
*Des*T442I	14.3	175	4.4
*Des*K449T	14.8	175	4.5
*Des*I451M	13.9	185	4.3
*Des*R454W	12.2	—[b]	4.0
*Des*S460I	16.5	190	4.6
*Des*V469M	14.9	200	4.2
*Des*WT + *Des*T442I	14.4	160	4.6
*Des*WT + *Des*K449T	12.8	180	3.9
*Des*WT + *Des*I451M	12.2	210	3.8
*Des*WT + *Des*R454W	12.9	180	4.1
*Des*WT + *Des*S460I	12.9	165	4.3
*Des*WT + *Des*V469M	13.7	185	4.2

[a] Filament diameters are average values from 100 measurements at different positions on an electronmicrograph of a single assembly. Standard deviation is typically 10%. Uncertainties are less than 5% for mesh size values and less than 10% for drag coefficient data.
[b] This mutation shows no plateau for mesh size calculation.

cytoplasmic IF networks, but nevertheless have the potential to express all network-constituting factors required.[13] In these cells, *Des*ΔTail and all mutants, except for *Des*R454W, were able to form filamentous networks comparable to those seen for wild-type desmin. *Des*R454W formed only short filamentous structures, which failed to fuse into a full network and were distributed all over the cytoplasm instead (Fig. 2a, right). Upon cotransfection with wild-type desmin, all mutants, including *Des*R454W (Fig. 2b, right) but excluding *Des*K449T formed filamentous networks. In combination with wild type desmin *Des*K449T gave rise to the formation of short filamentous particles and aggregates that were dispersed all over the cytoplasm (Fig. 2b, left). This correlates well with the observed assembly incompetence of the mixture of wild-type and *Des*K449T proteins *in vitro* (Fig. 1c, left). Second, in order to analyze the impact of a given mutation on authentic desmin networks, we employed cells derived from a mouse atrial cardiomyocyte lineage (HL-1).[17] In these cells, all mutants were able to integrate into the endogenous desmin network. Even *Des*K449T, which has been shown to exhibit a dominant-negative effect on wild-type desmin assembly upon cotransfection in vimentin-free cells, and *Des*R454W exhibited no obvious harmful effect on the endogenous HL-1 desmin cytoskeleton (data not shown). This might be explained by a low expression level of the mutant desmin or by the protective effect of cellular chaperones and confirms results previously obtained in C2C12 myoblast cells.[9]

Table 2. Persistence lengths, ranges, and numbers of assemblies and measurements

Protein	Average persistence length l_p (μm)	Persistence length range[a] (μm)	Number of assemblies/ measurements
Wild-type desmin (*Des*WT)	1.1	±0.5	18/28
*Des*ΔTail (c = 0.95 g/l)	0.7	0.7/0.7	1/2
*Des*T442I	2.0	±0.3	3/6
*Des*K449T	1.9	±0.6	3/7
*Des*I451M	1.7	±0.5	3/6
*Des*R454W	1.2[b]	1.0/1.1/1.4/1.4	2/4
*Des*S460I	1.4	1.3/1.4	2/2
*Des*V469M	1.9	±0.6	4/6
*Des*WT + *Des*T442I	1.2	1.2/1.2	1/2
*Des*WT + *Des*K449T	1.3	1.3/1.2	1/2
*Des*WT + *Des*I451M	1.1	1.0/1.1	1/2
*Des*WT + *Des*R454W	1.1	1.1/1.1	1/2
*Des*WT + *Des*S460I	1.0	1.0/1.0	1/2
*Des*WT + *Des*V469M	1.0	1.0/1.0	1/2

[a] For proteins for which at least three assemblies and at least six measurements were performed, standard deviation is denoted; in other cases, the individual results of each measurement are provided in this column.
[b] These filaments hardly form networks for which ξ could be determined, and we have used the mesh size of wild-type desmin as characteristic length scale for the calculation of l_p.

Linear viscoelastic filament and network response: Persistence length of filaments

The abovementioned studies suggest that tail mutants have an essentially preserved filament formation capacity both *in vitro* and in transfected cells. In order to prove our hypothesis that the mechanisms underlying the development of severe myopathy in affected patients could be sought in alterations in intrinsic filament properties, we investigated the mechanical properties of the filament networks. In the experimentally accessible frequency range $10 < \omega < 3 \times 10^4$ rad/s, we determined the linear viscoelastic shear moduli G' and G'' of protein solutions using high-frequency oscillatory squeeze flow experiments. In this range, the data exhibit $\omega^{3/4}$ scaling behavior, and we can calculate the persistence lengths of the single protein filament out of bulk solution measurements. The occurrence of $G \sim \omega^{3/4}$ has also been observed for F-actin solutions, but it takes place at significantly lower frequencies due to the higher stiffness of these filaments.[18,19]

Figure 3 shows the frequency dependence of the reduced loss modulus $(G'' - \omega\eta_s)/c$ on *Des*T442I solutions at protein concentrations between 0.5 g/l and 2.5 g/l. The moduli are divided by concentration, since linear concentration dependence is expected in the frequency range where internal relaxations of individual Kuhn segments dominate. This assumption is valid for concentrations up to 2 g/l, and there is no indication of a concentration-dependent structural change that would affect the bending stiffness of the desmin filaments. Accordingly, the G'' data superimpose fairly well for frequencies above 500 rad/s. The physical parameters required to calculate l_p are summarized in Table 1. The persistence length for this concentration series is $l_p = 2.0 \pm 0.3$ μm. For

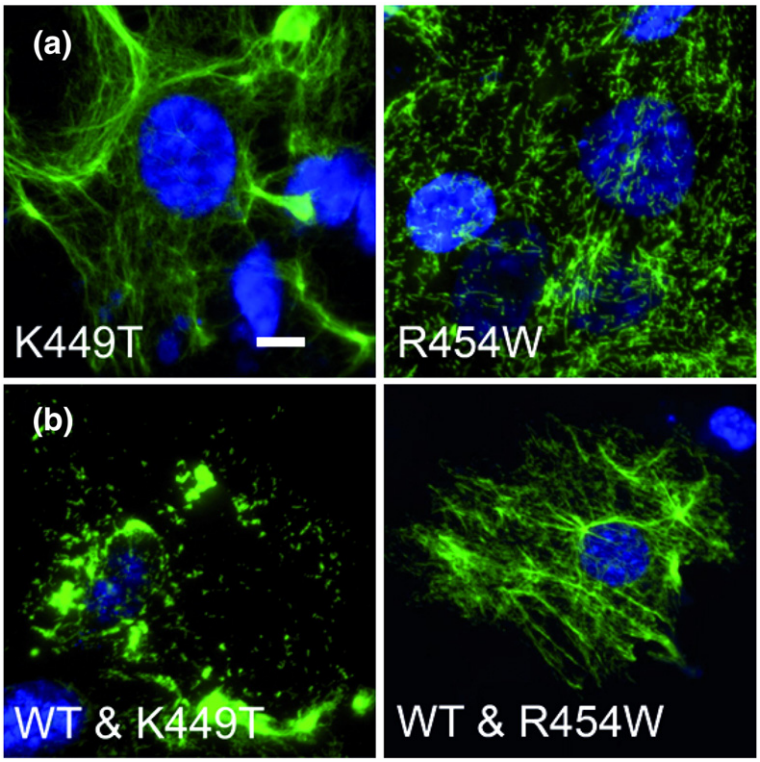

Fig. 2. Transfection studies in mouse embryonic fibroblasts (MEF $Vim^{-/-}$) devoid of endogenous cytoplasmic IF proteins (a and b). In fibroblast cells, *Des*K449T forms a network comparable to that of wild-type desmin (a; left). *Des*R454W forms only short filamentous structures that are distributed evenly across the cytoplasm (a; right). Upon cotransfection with wild-type desmin, *Des*K449T exhibits formation of intracellular aggregates (b; left). However, *Des*R454W can now assemble into normal filamentous networks (b; right). (a and b) Green, transfected desmin variant; blue, nuclear staining with 4,6-diamidino-2-phenylindole. Scale bar represents 10 μm.

$c = 2.5$ g/l, the reduced loss modulus is substantially higher compared to the other data for all frequencies, and no $\omega^{3/4}$ scaling is found in the frequency range investigated here.

In another set of experiments, we have determined the persistence lengths of pure wild-type and mutant desmin protein solutions (Fig. 4), as well as equimolar mixtures of wild-type and mutant desmin protein solutions (Fig. 5), from squeeze flow measurements at a single concentration of $c = 1.0$ g/l. All values are summarized in Table 2. Obviously, pure mutant desmin filaments exhibit some variation in their persistence length, and the lowest value (0.7 μm) is found for *Des*ΔTail. As can be seen from Tables 1 and 2, the mutants show a trend towards higher filament diameters and, correspondingly, higher stiffness; for heteropolymeric filaments, both filament diameter and persistence length are close to those of the wild type. However, there is no unique correlation between l_p and filament diameter. *Des*S460I, which has the highest filament diameter (16.5 nm), exhibits an intermediate stiffness with $l_p = 1.4$ μm, while *Des*ΔTail exhibits an IF diameter of 13.4 nm but the lowest stiffness (0.7 μm) among all investigated proteins. This indicates that bending stiffness is not solely controlled by cross-

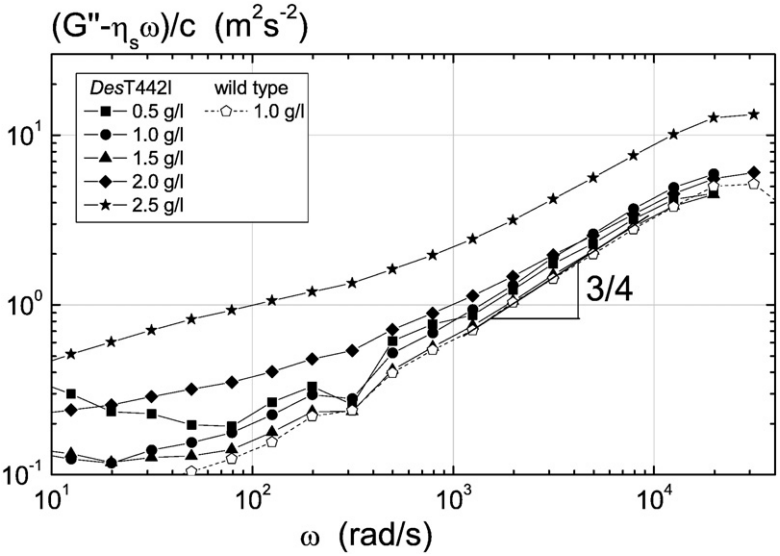

Fig. 3. Concentration dependence of the reduced linear viscoelastic loss modulus $G'' - \eta_s\omega$ of *Des*T442I, as determined from oscillatory squeeze flow measurements. $G'' - \eta_s\omega$ varies linearly with concentration up to $c = 2.0$ g/l at least in the frequency range between 10^3 rad/s and 10^4 rad/s, where $\omega^{3/4}$ scaling is observed. Thus, these data allow for a determination of the persistence length l_p according to Eq. (1).

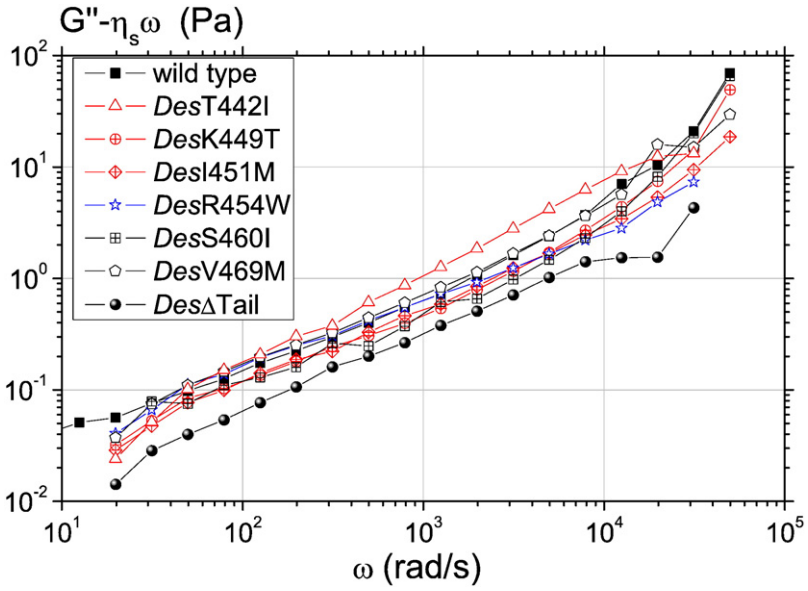

Fig. 4. The reduced linear viscoelastic loss modulus $G''-\eta_s\omega$ of *Des*T442I, *Des*K449T, *Des*I451M, *Des*R454W, *Des*S460I, and *Des*V469M, as well as wild-type desmin and *Des*ΔTail, as a function of frequency. The latter shows the lowest loss modulus values of all samples analyzed. The data for the other tail mutants range around those for wild-type desmin.

sectional diameter or mass distribution in the cross section, but presumably also by colloidal interactions along the filament and by the relative intrafilamentous mobility of individual strands along the filament axis ("axial slippage"). These observations indicate that a mutation in the tail domain of desmin can substantially alter not only the filament architecture but also intrafilamentous associations between individual subunits. This, in turn, has a direct effect on the bending stiffness of the filament. Of note, the absolute value of l_p obtained for a certain desmin sample was found to vary between different experiments due to subtle changes in sample preparation. These changes may influence network formation and alter, for example, the bundling of the filaments. For wild-type desmin, an average value $l_p = 1.1$ μm and a standard deviation of ±0.5 μm were determined from a series of 18 assemblies with 28 measurements. To minimize these effects, we dialyzed all proteins needed for a particular experiment and analyzed them on the same day. Within a given experimental day, the error was reduced to less than 10%.

Mesh size of filament networks

Previous experiments on wild-type desmin networks have shown that the linear viscoelastic storage modulus G' measured at a frequency of 1 rad/s can be identified as G_0. The corresponding ξ values for all samples are summarized in Table 1. This concept has not been applied to *Des*R454W, since this mutant hardly forms filament networks. The variation in G_0 is less than a factor of 2, indicating that the mutations obviously have only little effect on the number of cross-links/volume (i.e., mesh size).

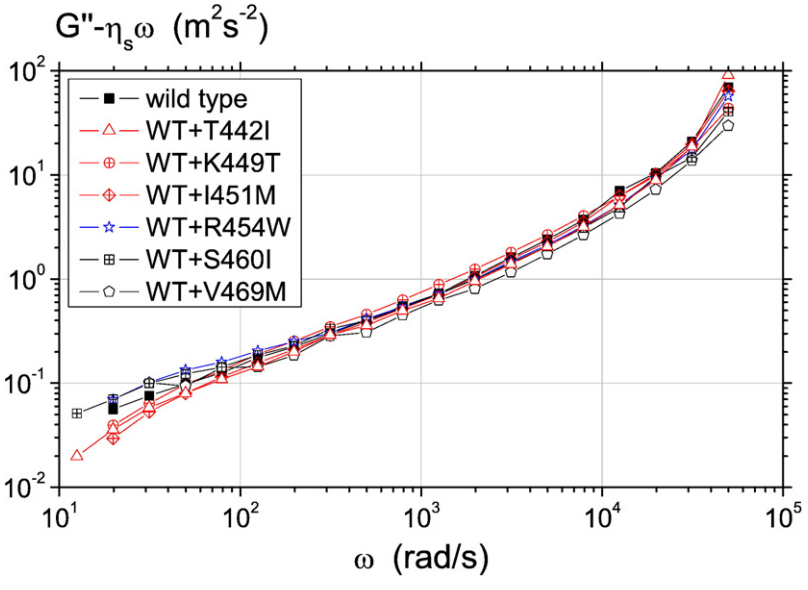

Fig. 5. The reduced linear viscoelastic loss modulus $G''-\eta_s\omega$ as a function of frequency for equimolar mixtures of each mutation with wild-type desmin. Data for the mixtures range closely around those for wild-type desmin.

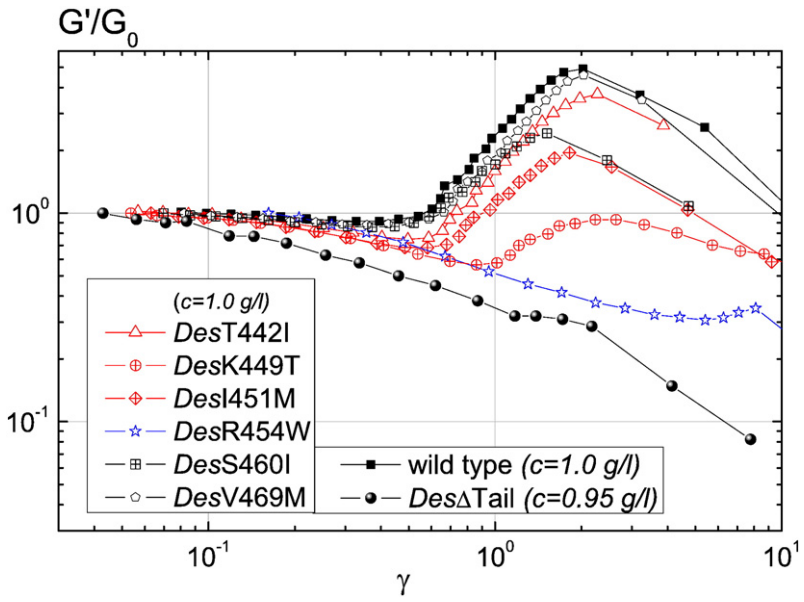

Fig. 6. The reduced storage modulus G'/G_0 of *Des*T442I, *Des*K449T, *Des*I451M, *Des*R454W, *Des*S460I, and *Des*V469M, as well as wild-type desmin and *Des*ΔTail networks, as a function of strain amplitude. Protein concentration is $c=1.0$ g/l, except for *Des*ΔTail, which has a concentration of $c=0.95$ g/l (this difference is not significant). Although assembly competent, *Des*ΔTail does not show strain stiffening in large-amplitude oscillatory shear experiments. *Des*R454W does not form extended filaments at all.

Nonlinear filament network deformation and rupture

Figure 6 plots the normalized storage modulus G'/G_0 as a function of strain amplitude at a fixed angular frequency $\omega=1$ rad/s for wild-type and mutant desmin filament networks normalized by the plateau modulus G_0. Figure 7 plots the storage modulus G' for the filament networks of equimolar mixtures of wild-type and mutant desmins. In all cases, the protein concentration c is kept constant at 1.0 g/l, except for *Des*ΔTail, where a slightly lower concentration ($c=0.95$ g/l) was employed. All samples exhibit linear viscoelastic behavior at strain amplitudes below $\gamma=0.1$ (i.e., G' is independent of γ). As pointed out in Mesh Size of Filament Networks, the absolute values of $G_0=\lim(\gamma\to0)G'$ are similar for all samples and lie in the range $0.5<G'<1.1$ Pa. For pure *Des*R454W and *Des*ΔTail, the storage modulus decreases monotonically with increasing strain amplitude. This is not surprising for *Des*R454W, as electron microscopy reveals that this mutant protein is not able to form extended filamentous networks (Fig. 1b). *Des*ΔTail, however, is capable of forming *bona fide* IFs (Fig. 1a), but the filamentous network does not exhibit strain stiffening under the ionic conditions employed. All other mutant proteins, as well as the mixtures with wild-type desmin, show substantial strain stiffening and exhibit a characteristic maximum in G' before the network breaks, and the apparent modulus eventually decreases when the sample loses contact with the upper cone of the rheometer. The critical strain amplitude γ_c at which strain stiffening sets lies between 0.5 and 0.9,

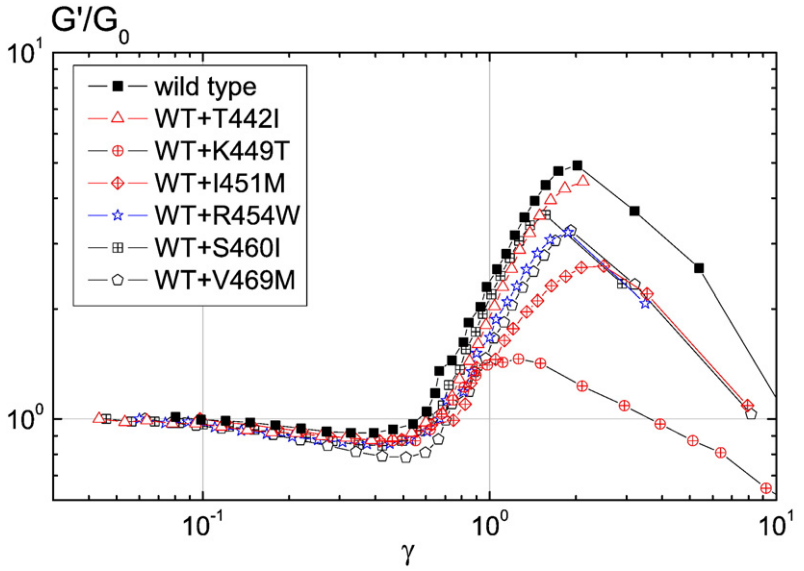

Fig. 7. The reduced storage modulus G'/G_0 of equimolar mixtures of wild-type desmin with the mutants *Des*T442I, *Des*K449T, *Des*I451M, *Des*R454W, *Des*S460I, and *Des*V469M at a protein concentration of $c=1.0$ g/l.

Table 3. Plateau modulus G_0 and ratio of maximum modulus G_{max} to G_0

Protein	Plateau modulus[a] G_0 (Pa)	G_{max}/G_0
Wild-type desmin	0.6±0.1	3.6±1.3
*Des*ΔTail (c=0.95 g/l)	0.2–1.0	No stiffening
*Des*T442I (c=1.0 g/l)	0.8–1.1	1.7–3.7
*Des*T442I (c=2.0 g/l)	1.6–1.8	14.0
*Des*K449T	0.8–1.0	0.8–0.9
*Des*I451M	0.5–0.9	1.2–2.0
*Des*R454W	No plateau	No stiffening
*Des*S460I	0.6–0.8	2.4–3.3
*Des*V469M	0.5–0.8	4.6–5.1
*Des*WT + *Des*T442I	1.0	4.4
*Des*WT + *Des*K449T	0.8	1.5
*Des*WT + *Des*I451M	0.5	2.6
*Des*WT + *Des*R454W	0.8	3.2
*Des*WT + *Des*S460I	1.0	3.6
*Des*WT + *Des*V469M	0.7	3.3

[a] Only for wild-type desmin with more than five assemblies standard deviation given. In other cases, the range of results is given if more than one assembly is performed. The typical relative accuracy of a single modulus measurement is about 5%.

whereas the strain amplitude γ_{max} at which the maximum in G' is reached is in the range of 1.5–2.5. The ratio of the maximum value of the storage modulus G_{max} to the linear viscoelastic modulus G_0 varies between G_{max}/G_0=0.8 for *Des*K449T and G_{max}/G_0=5.1 for *Des*V469M. For mixed systems, this ratio is always higher than that for the corresponding pure mutant proteins, except for *Des*V469M, and varies between $1.5<G_{max}/G_0<4.5$. Even *Des*R454W, which does not form a filament network itself (Fig. 1b), exhibits pronounced strain stiffening when combined with wild-type desmin, indicating that wild-type desmin can rescue the mechanical properties of the mutant protein. The weakest strain stiffening effect is observed for *Des*K449T, either assembled on its own or in combination with wild-type desmin. This corresponds to the assembly incompetence of the mixed proteins as observed by electron microscopy (Fig. 1c). All results for G_0 and G_{max}/G_0 are summarized in Table 3.

A closer inspection of the transition from linear viscoelastic response to nonlinear viscoelastic response reveals that G' goes through a minimum before strain stiffening sets in for all mutants and mixtures. This is in agreement with our findings for wild-type desmin[16] and might indicate nonaffine network deformation, as suggested previously by finite-element analysis of a two-dimensional network model.[20] This phenomenon seems to be characteristic of desmin, but is not observed for vimentin or other protein filament networks and is even more pronounced for the mutations and mixtures than for wild-type desmin (e.g., for *Des*K449T, the modulus drops to half of the corresponding G_0 value). For *Des*T442I, it is even observed at a concentration c=2 g/l, while it vanishes in the case of wild-type desmin for $c>1$ g/l. In summary, strain stiffening is equal or less pronounced, whereas the drop of the modulus before strain stiffening sets in is more pronounced for all mutations and mixtures than for the wild-type desmin.

Damage and rupture of desmin networks have been investigated by performing several consecutive stress amplitude sweep experiments on the same sample of fully assembled desmin filaments. The resulting dependence of G' (G'' shows similar characteristics; data not shown) on deformation amplitude for four subsequent measurements performed on a *Des*T442I desmin mutant solution with c=2.0 g/l is shown in Fig. 8. The first two sets of data acquisition are stopped before the maximum value of G' is reached. The deformation of the network is completely reversible for the first run. In the second run, γ is increased, but rupture of the network is not yet reached. However, this already leads to irreversible damage of the network structure since, in the third assessment of the sample, a small but significant drop of G' is observed. In this third run, stress

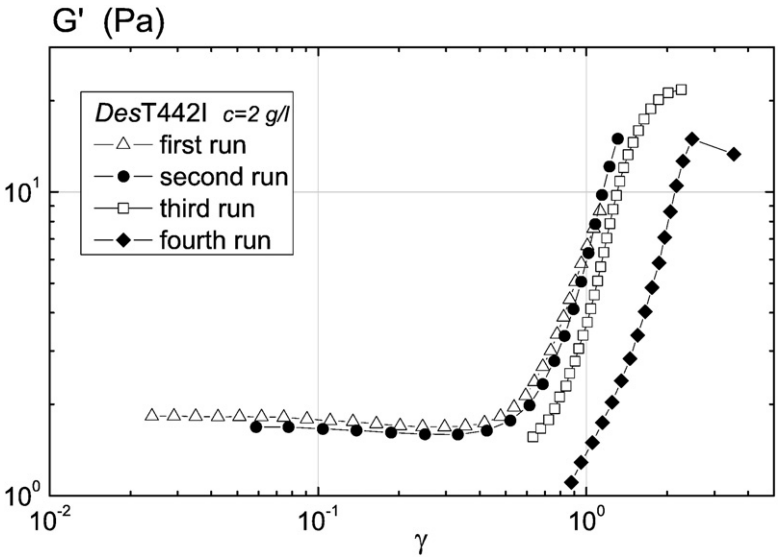

Fig. 8. Deformation dependence of the storage modulus G'/G_0 of a *Des*T442I desmin mutant solution with c=2.0 g/l. The moduli are shown for four subsequent measurements on the same sample. In the first two runs (triangles and circles), the maximum strain amplitude was chosen such that the maximum in G' had not yet been reached. The second run indicates the reversibility of strain stiffening for moderate deformations. In the third run (squares), stress has been increased to the point where G_{max} was reached. This clearly leads to a severe damage of the network structure, as can be seen from the drastic drop in G' observed in the fourth measurement (rhombi), but still, the network is strong enough to exhibit substantial strain stiffening.

has been increased to the point where the maximum in G' is reached, and this clearly leads to a severe damage of the network structure, as can be seen from the drastic drop in G' observed in the fourth measurement. Nevertheless, the network is still strong enough to exhibit substantial strain stiffening.

Conclusion

We have investigated the effect of mutations in the non-α-helical carboxy-terminal domain ("tail"). All mutants, with the exception of *Des*R454W, form *bona fide* filaments *in vitro* and in transfected cells. As long as a network is formed, the mutations do not have a significant effect on the shear modulus G_0 and, accordingly, on the mesh size of the network formed by the mutant protein. The various mutant desmin variants exhibit a persistence length on the same order of magnitude as wild-type desmin. We observe a trend towards growing stiffness with increasing filament diameter, but no unique correlation between these two quantities is found. Therefore, we presume that the flexibility of the filament is also affected by colloidal interactions along the filament and by axial slippage allowed between subfilamentous elements within the filament. The mutations can change the intrafilamentous architecture, thus causing an altered flexibility of the filaments. A similar effect has been observed by manipulation of individual filaments.[10] The strain stiffening properties of the mutant networks differ considerably from those of wild-type desmin. *Des*R454W does not form regular filament networks at all, but all other mutant proteins investigated here exhibit strain stiffening. However, except for *Des*V469M, it is always weaker than in the case of wild-type desmin. The importance of the non-α-helical tail domain for strain stiffening is pointed out by the complete absence of this property in the tail-truncated protein (*Des*ΔTail). Moreover, the minimum in G' observed at the onset of nonlinear stress response is more pronounced for mutations indicating a stronger nonaffine deformation (i.e., local variations of stress and strain fields under a large deformation). Strain stiffening is a well-known phenomenon for cross-linked semiflexible protein filament networks and has been reported for various other protein filament networks.[21–24] The degree of strain stiffening, as characterized by the slope of the G'-*versus*-γ curves and the G_{max}/G_0 ratio, is determined both by the flexibility of the filaments and by the bond strength of the network junctions. The balance between attractive and repulsive interactions again controls the latter. Obviously, this force equilibrium is strongly influenced by the "tail" domain of desmin. In particular, the tail-truncated protein forms a regular network, but does not show strain stiffening at all.

These findings prove our hypothesis that mutations in the desmin gene—although giving rise to the synthesis of mutant proteins that are assembly competent both *in vitro* and in transfected cells—can severely impact on the biophysical "intrinsic" filament properties. This results in slight changes in filament flexibility, but mainly in diminished stiffening of the filament network upon stress. We believe that these alterations in filament and network mechanics will influence the capacity of the extrasarcomeric desmin network to act in cellular mechanosensing, as well as in intracellular mechanotransduction pathways in patient muscle. Here, fine-tuned feedback loops regulate normal tissue function. Altered mechanical properties of part of this intricate machinery, as revealed by our analyses, will influence myocytes' capability to react to altered demands and thus may eventually cause myopathy. The relatively late onset of desminopathy points to the role of a changing complement of proteins in myocytes during aging that progressively alters the reaction of the cell towards the "mutated" filaments. Further studies will have to address this question in living cells and single muscle fibers isolated from transgenic mice carrying the corresponding mutated desmin.

Materials and Methods

Protein chemical methods

We selected mutations residing in desmin's non-α-helical carboxy-terminal "tail" domain for our rheological analyses, namely, *Des*T442I, *Des*K449T, *Des*I451M, *Des*R454W, *Des*S460I, and *Des*V469M. They have previously been characterized extensively.[9] In order to assess the role of the tail domain in desmin's viscoelastic properties, we generated a "tailless" desmin construct that terminates just after the highly conserved "…TYRKLLEGEESRI-416" motif at the end of coil 2B of desmin's α-helical "rod" domain (*Des*ΔTail). *Escherichia coli* strain TG1 (Amersham, Germany) was transformed with human wild-type and mutant desmin plasmids, respectively. Recombinant proteins were purified from inclusion bodies, as described previously.[24,25] For *in vitro* reconstitution of purified recombinant proteins, up to 4.0 g/l protein was dialyzed out of 8 M urea and 10 mM Tris–HCl (pH 7.5) into a buffer containing 5 mM Tris–HCl (pH 8.4), 1 mM ethylenediaminetetraacetic acid, 0.1 mM ethylene glycol bis(*b*-aminoethyl ether) *N*,*N*′-tetraacetic acid, and 1 mM DTT ("Tris buffer") using regenerated cellulose dialysis tubing (molecular weight cutoff, 50,000; Spectra/Por®; Roth, Germany). Filament assembly was initiated by addition of an equal volume of "assembly buffer" [45 mM Tris–HCl (pH 7.0) and 100 mM NaCl, at 37 °C]. For mixing experiments, equimolar amounts of desmin and the respective mutant protein were combined in 9.5 M urea prior to dialysis into "Tris buffer" in order to allow heteropolymerization from the dimer level onwards.[25]

For rheological measurements, protein solutions were filled into the preheated sample cell directly after initiation of assembly, and gap height was immediately set. After 30 min, measurements were started. This polymerization time had been established in previous analyses.[16]

Electron microscopy

As described previously, we assembled the proteins at a concentration of $c = 1.0$ g/l.[16] Prior to absorption to the

formvar-coated grid, samples were diluted to a concentration of $c = 0.1$ g/l. After negative staining, micrographs of the specimens were recorded as described previously.[25,26] The images were scanned and evaluated with the free software ImageJ 1.32j (National Institutes of Health, Bethesda, MD, USA‡). For assessment of filament diameters, at least 100 filament widths were measured. Further details can be found in Schopferer *et al.*[16]

Cell culture and microscopic procedures

For transfection studies, we employed a cell line completely devoid of cytoplasmic IFs, namely, early-passage primary fibroblast cultures of vimentin knockout ($Vim^{-/-}$) mouse embryos ($MEF^{-/-}$).[27] In order to assess the potential of the mutant desmin variants to integrate into a preexisting cytoplasmic IF system, we employed a murine cardiac muscle cell line that expresses endogenous desmin (HL-1).[17] Cells were plated on glass coverslips placed in six-well plates for 1–2 days, grown to ~30% confluency, and then transiently transfected with 5 μg of plasmid DNA per plate using Fugene 6® in accordance with the manufacturer's protocol (Roche Diagnostics, Germany). Forty-eight hours after transfection, cells were processed for immunocytochemistry. Briefly, cells were fixed in methanol for 5 min, followed by permeabilization in acetone for 3 min at −20 °C. HL-1 cells were cotransfected with a construct coding for lamin B1 and the respective desmin constructs. These cells were washed with phosphate-buffered saline (PBS) containing 2 mM $MgCl_2$ and fixed with freshly prepared 4% formaldehyde in PBS on ice for 7 min. After fixation, these latter cells were washed with PBS containing 2 mM $MgCl_2$, permeabilized with 0.1% Triton X-100 in PBS for 5 min on ice, and finally washed with PBS containing 2 mM $MgCl_2$. Irrespective of the abovementioned fixation protocol, specimens were blocked for 30 min in 10% donkey serum in PBS after rehydration. The coverslips were then incubated with the polyclonal rabbit anti-desmin serum (dilution 1:100; Progen, Germany) together with the monoclonal anti-vimentin antibody Vim3B4 (undiluted; Progen) for 60 min at room temperature. After a thorough rinsing in PBS, Cy-3-labeled donkey–anti-mouse antibody (dilution 1:300; Dianova, Germany) and Alexa-488-labeled donkey–anti-rabbit antibody (dilution 1:100; Invitrogen, Germany) were applied simultaneously for 30 min together with 4,6-diamidino-2-phenylindole (dilution 1:1000; Roche Diagnostics) for nuclear staining. The coverslips were finally mounted on glass slides in Fluoromount G (Southern Biotechnology Associates, USA). Cells were viewed by confocal laser scanning fluorescence microscopy (DMIRE 2; Leica, Germany).

Rheology

Low-frequency measurements

With the commercial rheometer Haake RheoScope1 (Haake, Karlsruhe, Germany), we measured the storage modulus G' and the loss modulus G'' as described previously.[16] Briefly, cone and plate geometry was employed to perform oscillatory stress amplitude sweep experiments in order to characterize nonlinear material response. At a fixed frequency of $\omega = 1$ rad/s, the stress amplitude τ was varied between 10^{-2} Pa and 10 Pa. G' and G'' were calculated from the amplitude and the phase shift of the response signal. At low stresses in the linear response regime, the moduli G' and G'' are calculated from the in-phase and out-of-phase sinusoidal deformation signals. At larger deformations, the response signal differs from pure sinusoidal excitation. Then G' and G'' are calculated from the amplitude and the phase shift of the response signal according to a company proprietary algorithm based on fast Fourier transform methods including the third and fifth harmonics of the applied frequency; thus, data have to be treated as apparent moduli.

High-frequency measurements

For characterization of the linear viscoelastic response of protein filaments at frequencies beyond 100 rad/s, we apply oscillatory squeeze flow using a piezoaxial vibrator apparatus in accordance with published methods.[28,29] We performed oscillatory frequency sweep experiments at low amplitudes. The device provides a frequency range of $10^1 < \omega < 5 \times 10^4$ rad/s. All measurements were conducted at a temperature of 37 °C.

Persistence length of filaments

As shown previously, the persistence length or, equivalently, the bending stiffness of IFs can be determined from the abovementioned linear viscoelastic moduli $G^* = G' + iG''$.[16] Briefly, semiflexible IFs exhibit a distinct scaling behavior of $G^* \sim \omega^{3/4}$ within a characteristic frequency regime of internal molecular relaxations.[30] The absolute value of G^* is related to the persistence length l_p and therefore characterizes the flexibility of the filament chain:[31]

$$G^* - i\omega\eta_s = \frac{1}{15}\rho\kappa l_p\left(\frac{-2i\zeta}{\kappa}\right)^{3/4}\omega^{3/4} \qquad (1)$$

Here we use the imaginary part of Eq. (1) (i.e., the loss modulus G'') in order to determine l_p, since this quantity is determined more accurately with our squeeze flow apparatus than G'. The details and assumptions of this calculations can be found in our previous work.[16]

Mesh size of network

A characteristic frequency range where G' is much larger than G'' and independent of frequency is typical of polymer networks. Correspondingly, the value of G' is called plateau modulus G_0. The theory of classical entropy (rubber) elasticity[20] relates the plateau modulus directly to the cross-link density ν of the network: $G_0 = \nu k_B T$. In a homogeneous network, the mesh size ξ of that network can be calculated from the value of G_0 via $\xi = \sqrt[3]{kT / G_0}$.

‡ http://rsb.info.nih.gov/ij

Acknowledgements

H. Bär and H. Herrmann acknowledge grants from the German Research Foundation (BA 2186/2-1 to H.B., HE 1853 to H.H., and BA 2186/3-1 to H.B. and H.H.).

References

1. Herrmann, H., Bär, H., Kreplak, L., Strelkov, S. V. & Aebi, U. (2007). Intermediate filaments: from cell architecture to nanomechanics. *Nat. Rev. Mol. Cell Biol.* **8**, 562–573.
2. Goldfarb, L., Olive, M., Vicart, P. & Goebel, H. H. (2008). Intermediate filament diseases: desminopathy. *Adv. Exp. Med. Biol.* **642**, 131–164.
3. Goldfarb, L. G., Park, K. Y., Cervenakova, L., Gorokhova, S., Lee, H. S., Vasconcelos, O. *et al.* (1998). Missense mutations in desmin associated with familial cardiac and skeletal myopathy. *Nat. Genet.* **19**, 402–403.
4. Munoz-Marmol, A. M., Strasser, G., Isamat, M., Coulombe, P. A., Yang, Y., Roca, X. *et al.* (1998). A dysfunctional desmin mutation in a patient with severe generalized myopathy. *Proc. Natl Acad. Sci. USA*, **95**, 11312–11317.
5. Goldfarb, L. G., Vicart, P., Goebel, H. H. & Dalakas, M. C. (2004). Desmin myopathy. *Brain*, **127**, 723–734.
6. Bär, H., Kostareva, A., Sjöberg, G., Sejersen, T., Katus, H. A. & Herrmann, H. (2006). Forced expression of desmin and desmin mutants in cultured cells: impact of myopathic missense mutations in the central coiled-coil domain on network formation. *Exp. Cell Res.* **312**, 1554–1565.
7. Bär, H., Mücke, N., Kostareva, A., Sjöberg, G., Aebi, U. & Herrmann, H. (2005). Severe muscle disease-causing desmin mutations interfere with *in vitro* filament assembly at distinct stages. *Proc. Natl Acad. Sci. USA*, **102**, 15099–15104.
8. Bär, H., Mücke, N., Ringler, P., Müller, S. A., Kreplak, L., Katus, H. A. *et al.* (2006). Impact of disease mutations on the desmin filament assembly process. *J. Mol. Biol.* **360**, 1031–1042.
9. Bär, H., Goudeau, B., Wälde, S., Casteras-Simon, M., Mücke, N., Shatunov, A. *et al.* (2007). Conspicuous involvement of desmin tail mutations in diverse cardiac and skeletal myopathies. *Hum. Mutat.* **28**, 374–386.
10. Kreplak, L. & Bär, H. (2009). Severe myopathy mutations modify the nanomechanics of desmin intermediate filaments. *J. Mol. Biol.* **385**, 1043–1051.
11. Conover, G. M., Henderson, S. N. & Gregorio, C. C. (2009). A myopathy-linked desmin mutation perturbs striated muscle actin filament architecture. *Mol. Biol. Cell*, **20**, 834–845.
12. Ma, L., Yamada, S., Wirtz, D. & Coulombe, P. A. (2001). A 'hot-spot' mutation alters the mechanical properties of keratin filament networks. *Nat. Cell Biol.* **3**, 503–506.
13. Bousquet, O., Ma, L., Yamada, S., Gu, C., Idei, T., Takahashi, K. *et al.* (2001). The nonhelical tail domain of keratin 14 promotes filament bundling and enhances the mechanical properties of keratin intermediate filaments *in vitro*. *J. Cell Biol.* **155**, 747–754.
14. Lee, C. -H. & Coulombe, P. A. (2009). Self-organization of keratin intermediate filaments into cross-linked networks. *J. Cell Biol.* **186**, 409–421.
15. Herrmann, H., Häner, M., Brettel, M., Ku, N. -O. & Aebi, U. (1999). Characterization of distinct early assembly units of different intermediate filament proteins. *J. Mol. Biol.* **286**, 1403–1420.
16. Schopferer, M., Bär, H., Hochstein, B., Sharma, S., Mücke, N., Herrmann, H. & Willenbacher, N. (2009). Desmin and vimentin intermediate filament networks: their viscoelastic properties investigated by mechanical rheometry. *J. Mol. Biol.* **388**, 133–143.
17. Claycomb, W. C., Lanson, N. A., Jr., Stallworth, B. S., Egeland, D. B., Delcarpio, J. B., Bahinski, A. & Izzo, N. J., Jr (1998). HL-1 cells: a cardiac muscle cell line that contracts and retains phenotypic characteristics of the adult cardiomyocyte. *Proc. Natl Acad. Sci. USA*, **95**, 2979–2984.
18. Gisler, T. & Weitz, D. A. (1999). Scaling of the microrheology of semidilute F-actin solutions. *Phys. Rev. Lett.* **82**, 1606.
19. Xu, J., Palmer, A. & Wirtz, D. (1998). Rheology and microrheology of semiflexible polymer solutions: actin filament networks. *Macromolecules*, **31**, 6486–6492.
20. Onck, P. R., Koeman, T., van Dillen, T. & van der Giessen, E. (2005). Alternative explanation of stiffening in cross-linked semiflexible networks. *Phys. Rev. Lett.* **95**, 178102–178104.
21. Janmey, P., Euteneuer, U., Traub, P. & Schliwa, M. (1991). Viscoelastic properties of vimentin compared with other filamentous biopolymer networks. *J. Cell Biol.* **113**, 155–160.
22. Gardel, M. L., Shin, J. H., MacKintosh, F. C., Mahadevan, L., Matsudaira, P. & Weitz, D. A. (2004). Elastic behavior of cross-linked and bundled actin networks. *Science*, **304**, 1301–1305.
23. Coulombe, P. A., Bousquet, O., Ma, L., Yamada, S. & Wirtz, D. (2000). The 'ins' and 'outs' of intermediate filament organization. *Trends Cell Biol.* **10**, 420–428.
24. Rammensee, S., Janmey, P. A. & Bausch, A. R. (2007). Mechanical and structural properties of *in vitro* neurofilament hydrogels. *Eur. Biophys. J.* **36**, 661–668.
25. Bär, H., Fischer, D., Goudeau, B., Kley, R. A., Clemen, C. S., Vicart, P. *et al.* (2005). Pathogenic effects of a novel heterozygous R350P desmin mutation on the assembly of desmin intermediate filaments *in vivo* and *in vitro*. *Hum. Mol. Genet.* **14**, 1251–1260.
26. Hofmann, I., Herrmann, H. & Franke, W. W. (1991). Assembly and structure of calcium-induced thick vimentin filaments. *Eur. J. Cell Biol.* **56**, 328–341.
27. Holwell, T. A., Schweitzer, S. C. & Evans, R. M. (1997). Tetracycline regulated expression of vimentin in fibroblasts derived from vimentin null mice. *J. Cell Sci.* **110**, 1947–1956.
28. Kirschenmann, L. (2003). Aufbau zweier piezoelektrischer Sonden (PRV/PAV) zur Messung der viskoelastischen Eigenschaften weicher Substanzen im Frequenzbereich 0.5 Hz–2 kHz bzw. 0.5 Hz–7 kHz. PhD dissertation, Ulm.
29. Crassous, J. J., Regisser, R., Ballauff, M. & Willenbacher, N. (2005). Characterization of the viscoelastic behavior of complex fluids using the piezoelastic axial vibrator. *J. Rheol.* **49**, 851–863.
30. Morse, D. C. (1998). Viscoelasticity of tightly entangled solutions of semiflexible polymers. *Phys. Rev. E*, **58**, R1237–R1240.
31. Gittes, F. & MacKintosh, F. C. (1998). Dynamic shear modulus of a semiflexible polymer network. *Phys. Rev. E*, **58**, R1241–R1244.